LBL-36883
UC-414

To be published in the Proceedings of the Eleventh International Conference on
Ultra-Relativistic Nucleus-Nucleus Collisions (Quark Matter '95),
Monterey, California, January 9-13, 1995,
Nuclear Physics A

First Results from NA49 on Pb+Pb Collisions at 158 GeV/Nucleon

Spiros Margetis
Lawrence Berkeley Laboratory
University of California, Berkeley, CA 94720

and

the NA49 Collaboration

March 1995

This work was supported by the Director, Office of Energy Research, Division of Nuclear Physics of the Office of High Energy and Nuclear Physics of the U.S. Department of Energy under Contract DE-AC03-76SF00098

First Results from NA49 on Pb+Pb Collisions at 158 GeV/Nucleon

S. Margetis and the NA49 Collaboration

T. Alber[13], H. Appelshäuser[7], J. Bächler[9], J. Bartke[6], H. Białkowska[14], F. Bieser[2], M.A. Bloomer[2], C.O. Blyth[3], R. Bock[7], C. Bormann[9], F.P. Brady[8], R. Brockmann[7], P. Buncic[5,7], H.L. Caines[3], D. Cebra[8], P. Chan[16], G. Cooper[2], J.G. Cramer[16,13], P.B. Cramer[16], P. Csato[4], I. Derado[13], J. Dunn[8], V. Eckardt[13], F. Eckhardt[12], S. Euler[12], M.I. Ferguson[5], H.G. Fischer[5], Z. Fodor[4], P. Foka[7], P. Freund[13], M. Fuchs[7], J. Gal[4], M. Gaździcki[9], E. Gładysz[6], J. Grebieszkow[14], J. Günther[9], J.W. Harris[2], W. Heck[10], S. Hegyi[4], L.A. Hill[3], I. Huang[8], M.A. Howe[16], G. Igo[11], D. Irmscher[2], P. Jacobs[2], P.G. Jones[3], K. Kadija[17,13], J. Kecskemeti[4], J. Kosiec[15], M. Kowalski[6], A. Kühmichel[5], B. Lasiuk[11], S. Margetis[2], J.W. Mitchell[8], A. Mock[13], J.M. Nelson[3], G. Odyniec[2], J. Palinkas[4], G. Palla[4], A.D. Panagiotou[1], A. Petridis[1,13], A. Piper[12], A.M. Poskanzer[2], D.J. Prindle[16], F. Pühlhofer[12], W. Rauch[13], R. Renfordt[9,5], W. Retyk[14], H.G. Ritter[2,5], D. Röhrich[9], H. Rudolph[2], K. Runge[10], A. Sandoval[7], H. Sann[7], E. Schäfer[13], N. Schmitz[13], S. Schönfelder[13], P. Seyboth[13], J. Seyerlein[13], F. Sikler[4], E. Skrzypczak[15], P. Stefański[6], R. Stock[9], H. Ströbele[9], I. Szentpetery[4], J. Szikłai[4], M. Toy[2,11], T.A. Trainor[16], S. Trentalange[11], M. Vassiliou[1,13], G. Vesztergombi[4], D. Vranic[7,17], S. Wenig[5], C. Whitten[11], T. Wienold[2], L. Wood[8], J. Zimanyi[4], X.-Z. Zhu[16], R. Zybert[3]

[1] Department of Physics, University of Athens, Athens, Greece, [2] Lawrence Berkeley Laboratory, University of California, Berkeley, USA, [3] Birmingham University, Birmingham, England, [4] Institute of Physics, Budapest, Hungary, [5] CERN, Geneva, Switzerland, [6] Institute of Nuclear Physics, Cracow, Poland, [7] Gesellschaft für Schwerionenforschung (GSI), Darmstadt, Germany, [8] University of California at Davis, Davis, USA, [9] Fachbereich Physik der Universität, Frankfurt, Germany, [10] Fachbereich Physik der Universität, Freiburg, Germany, [11] University of California at Los Angeles, Los Angeles, USA, [12] Fachbereich Physik der Universität, Marburg, Germany, [13] Max-Planck-Institut für Physik, Munich, Germany, [14] Institute for Nuclear Studies, Warsaw, Poland, [15] Institute for Experimental Physics, University of Warsaw, Warsaw, Poland, [16] Nuclear Physics Laboratory, University of Washington, Seattle, WA, USA, [17] Rudjer Boskovic Institute, Zagreb, Croatia

First results from the NA49 experiment with a ^{208}Pb beam on a Pb target at the CERN SPS with total energy of 33 TeV are presented. Data on transverse energy production, forward energy flow and rapidity density of negative hadrons are shown and discussed. The degree of nuclear stopping and the energy densities achieved are estimated for near head-on collisions.

1. Experiment NA49

The NA49 experiment is designed to perform inclusive as well as single event measurements of a variety of observables for ^{208}Pb induced reactions at 158 GeV/nucleon

CERN EXPERIMENT NA49

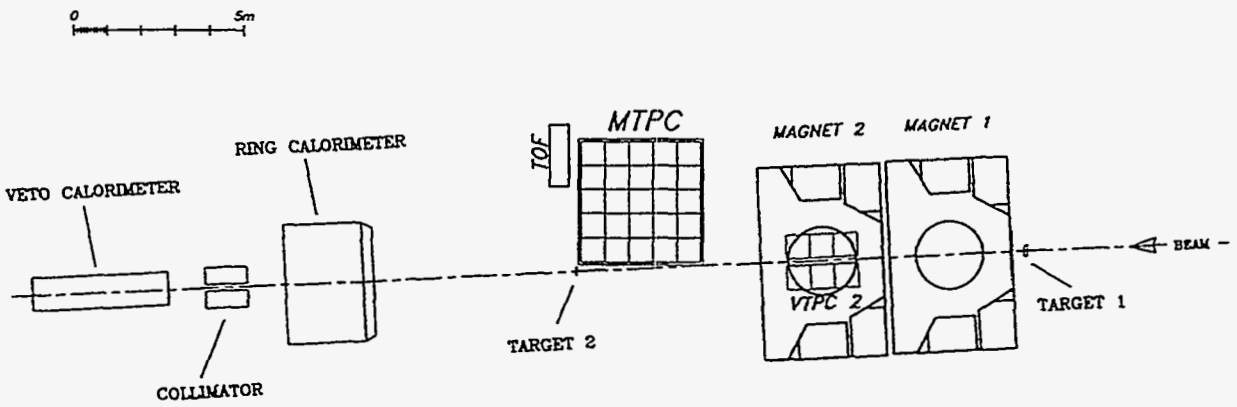

Figure 1. Top view of the NA49 experimental setup in its 1994 run configuration.

laboratory energy. Its partially completed 1994 run configuration (Fig. 1) included two large volume Time Projection Chambers (TPCs) as tracking devices, a Time Of Flight system (TOF), and a set of Calorimeters for transverse (E_T) and forward (E_{VETO}) energy flow measurements. The beam is defined by a 0.2 mm quartz Cherenkov counter followed by a veto scintillator counter with a 10 mm central hole. For the TPC runs, a thin target was placed at the entrance to the first magnet, and for the E_T measurements, 6 meters upstream of the face of the Ring Calorimeter. Two Vertex Magnets with a total bending power of up to 9 T·m are used for the momentum analysis of the produced charged particles. One TPC is placed inside the downstream magnet(VTPC2), the other (MTPC) in the field–free region behind the magnets.

A 'Ring' Calorimeter[1] covers the pseudorapidity region $2.1 < \eta < 3.4$ for particles produced in target–2. It consists of an electromagnetic Lead/Scintillator calorimeter 16 radiation lengths (X_0) and 1 interaction length (λ_{int}) thick, followed by a hadronic Iron/Scintillator calorimeter of 6 λ_{int}. It is tube-shaped with an inner/outer radius of 0.28/1.50 meters, and it is divided into 240 cells, 24 in azimuth and 10 radially with the radial size chosen so as to cover equal units in pseudorapidity.

Behind the Ring Calorimeter an iron collimator defines the acceptance of the forward ('Veto') calorimeter[1]. Its hole of 10x10 cm^2 at 11 meters from target–2 allows only particles with an emission angle of less than about 0.3^0 ($\approx 5^0$ in the c.m. frame) to reach the Veto calorimeter. This small solid angle covers the projectile spectator region.

Two different types of triggers were used for the data presented here: an unbiased trigger (calorimeter runs only), where the only requirement was a valid beam particle, and a Veto trigger where not only a valid beam particle was required but also an energy deposition in the Veto calorimeter below a certain amount.

2. Data Analysis

Both calorimeters have been used in previous experiments (NA5, NA24, NA35) and their behavior has been studied in detail [4]. For the ^{208}Pb beam runs the gain of the phototubes in the inner six rings had to be reduced by a factor up to 3 in order to avoid signal overflows [2]. Three sectors (30 cells) were re-calibrated using 30 GeV π^- and e^- beams. The rest were tuned by using ^{208}Pb+Pb data assuming azimuthal symmetry, on the average, for E_T. The e/π ratio for the EM part is found to be 1.4 at 30 GeV and the energy resolution for electromagnetic (hadronic) showers in the Ring Calorimeter is $\sigma(E)/E = 30(100)\%/\sqrt{E}$, respectively.

The Veto calorimeter is placed about 20 meters downstream of the last beam counter, therefore beam interactions with air as well as some other material placed in the beam's path were unavoidable. This leads to a high rate of non-target interactions, which mimic peripheral collisions in the case of minimum bias runs. In order to have a reasonable fraction of target interactions in the recorded data for the unbiased runs, we used targets with thicknesses of up to 10% nuclear interaction length for ^{208}Pb projectiles. Otherwise, the nominal calorimeter target thickness is 2% of λ_{int}^{Pb}. All the TPC data are virtually background free due to the strict Veto trigger requirements.

The typical cell occupancy for central Pb+Pb events is up to about 5 particles/cell, and a typical hadronic shower in the Calorimeter occupies up to 8 neighboring cells, so that individual showers cannot be reconstructed. The effect of the shower spreading over several cells combined with the non-projective geometry of the calorimeter was estimated through a Monte Carlo study and applied to the data. Non–compensating hadron calorimeters have a non–linear response to hadrons of low energy (< 5 GeV). Since a large fraction of the produced particles are in that energy range (up to about 30% in the outer ring according to event generators), a correction factor was estimated and applied to the signal of the Hadron part.

On the average about 95% of the electromagnetic energy, mostly coming from the gammas of the neutral pion decays, is contained in the EM part. Since it represents a thickness of one λ_{int}, depending upon the radial position, also a fraction between 35–65% of the incident hadronic energy is deposited in it, representing about 50% of its total response. The deposited fraction was estimated for central collisions with the help of an event generator and a GEANT simulation of the calorimeter. For the evaluation of the electromagnetic and hadronic components in an event, the estimated hadronic signal in the EM part was subtracted from its total response. The estimated hadronic signal was multiplied with the e/π factor of the EM part, and added to the hadronic energy. This manipulation of large fractions of the EM signal is responsible for the systematic uncertainty in the estimation of the individual components of the total transverse energy.

The systematic error in the total E_T scale is estimated to be 10%, and for the E_T^{EM}, E_T^{HAD} scale approximately 15%. The systematic error on the cross section scales is estimated to be less than 10% which is mainly due to uncertainties on the amount of contamination of the beam arriving at the calorimeter target.

The single particle spectra and particle correlations are measured using the two TPCs: VTPC2 and MTPC (fig. 1). The VTPC2 registers up to 72 and the MTPC up to 90 charge clusters along the particle trajectory. The clusters are used for the reconstruction of the

space points on the trajectory with typical resolution of about 300 microns. Both TPCs cover a similar angular–momentum region, which allows the analsis of pion production above midrapidity ($y_{cm} = 2.9$) and proton production around midrapidity. The VTPC2 in addition allows the study of neutral strange particle production, whereas the MTPC is able to perform statistical identification of charged particles using ionization information. The data sample for the results presented here consists of about 250000 calorimeter events and 100 TPC events.

3. Results

The correlation between the forward flowing energy, E_{VETO}, as seen by the Veto calorimeter, and the produced transverse energy, E_T, around midrapidity, in the Ring calorimeter's acceptance ($2.1 < \eta < 3.4$) is shown in Fig. 2a. We observe an anticorrelation between the two quantities, i.e. almost zero E_T at the full beam energy (≈ 33 TeV) and large values of E_T (≈ 0.5 TeV) for the lowest E_{VETO}. This can be understood in the

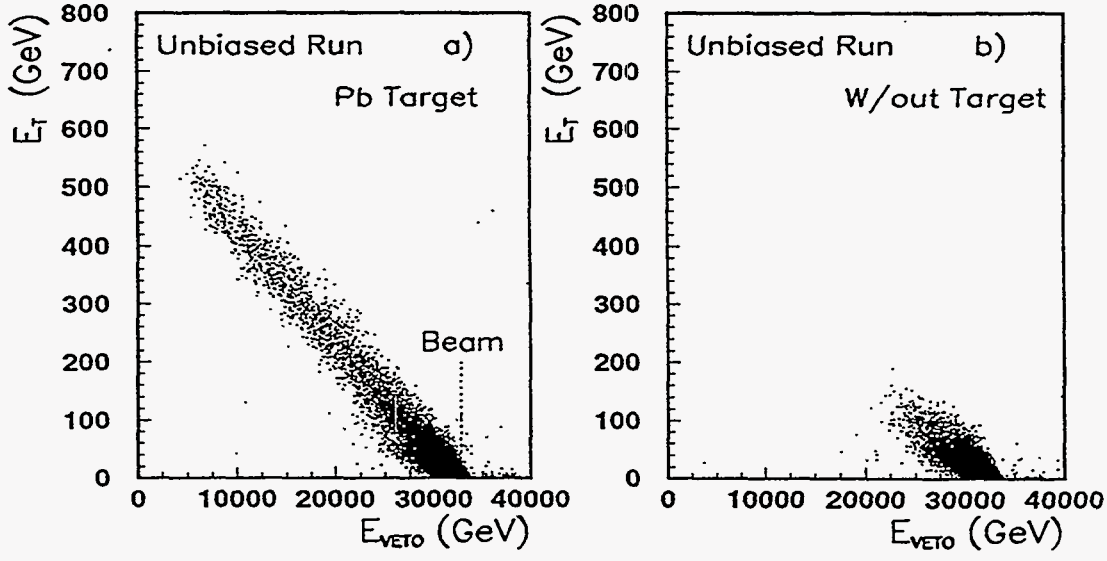

Figure 2. Correlation between E_{VETO} and E_T. Each plot represents about 40000 triggers.

framework of a participant–spectator model: for decreasing values of impact parameter the number of spectators decreases as the number of participants increases. Transverse energy is produced by redistribution in phase-space of the initial longitudinal momentum of the participant nucleons and increases with the number of participants, whereas the forward energy is mostly spectator energy for most impact parameters. We therefore understand the qualitative features of this figure to be governed primarily by the collision geometry, as intuitively expected. Figure 2b shows the same correlation plot with the same trigger conditions but with the target removed. This was done in order to under-

stand the effect of the non-target interactions on the measured spectra. We see that the low atomic number material in the beam's path (mostly air, C and Al) can only influence the E_T spectra up to 200 GeV and the E_{VETO} down to about 23 TeV. The high E_T (or low E_{VETO}) part of the spectra is background free. After each calorimeter run data were taken without the target and the non-target interaction spectra were subtracted after normalization.

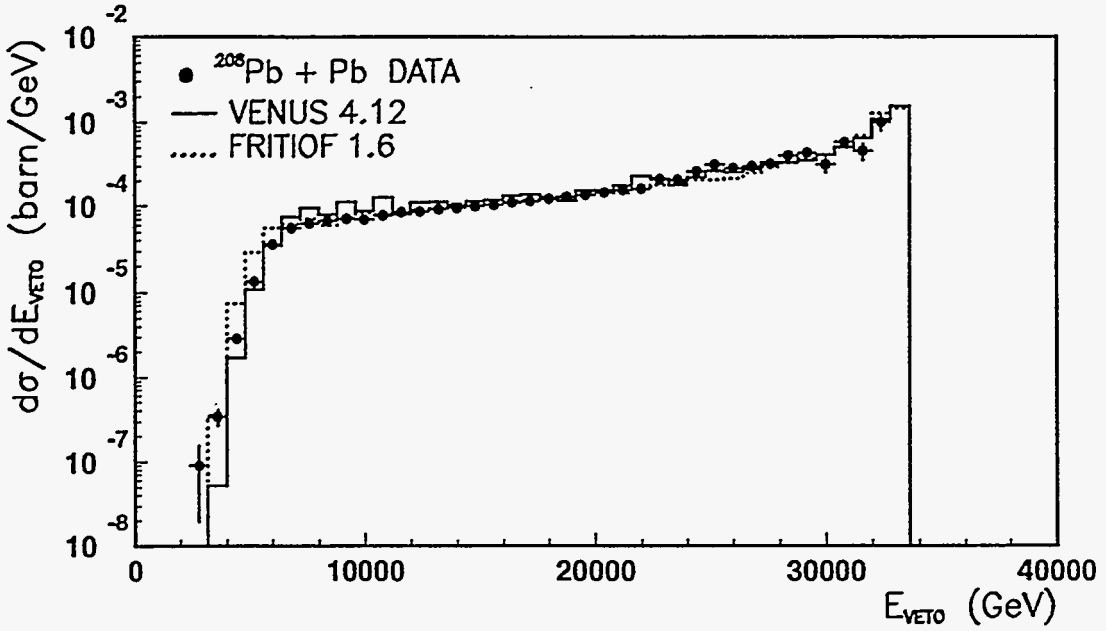

Figure 3. Differential cross section distributions of the energy measured in the Veto calorimeter. Predictions of FRITIOF and the VENUS models are also shown.

In Fig. 2a we also observe that in this symmetric collision system, even for the smallest possible impact parameters, a fraction of the initial beam energy reaches the Veto Calorimeter. In order to understand this in a more quantitative way we plot the E_{VETO} distribution in Fig. 3. The spectrum reflects the collision geometry: large values of cross section for large impact parameters, around the full beam energy, followed by a plateau for a large range of impact parameters, where the two nuclei partially overlap, and rapidly vanishing cross sections for low E_{VETO} values. String model predictions, VENUS and FRITIOF[1], closely reproduce the features of the data, thus underlining the validity of the collision geometry picture.

Central, near zero impact parameter, collisions have a mean energy deposition in the Veto calorimeter of about 6 TeV, corresponding to the point in the E_{VETO} spectrum where the plateau ends and the steep fall of the cross section starts. Simple calculations of the collision geometry show that even head–on collisions have 13±2 projectile spectators

[1]Fritiof's JETSET parameters #2, 12 and 52 were modified so that the model could reproduce the NA35 S+S data on strangeness and stopping.

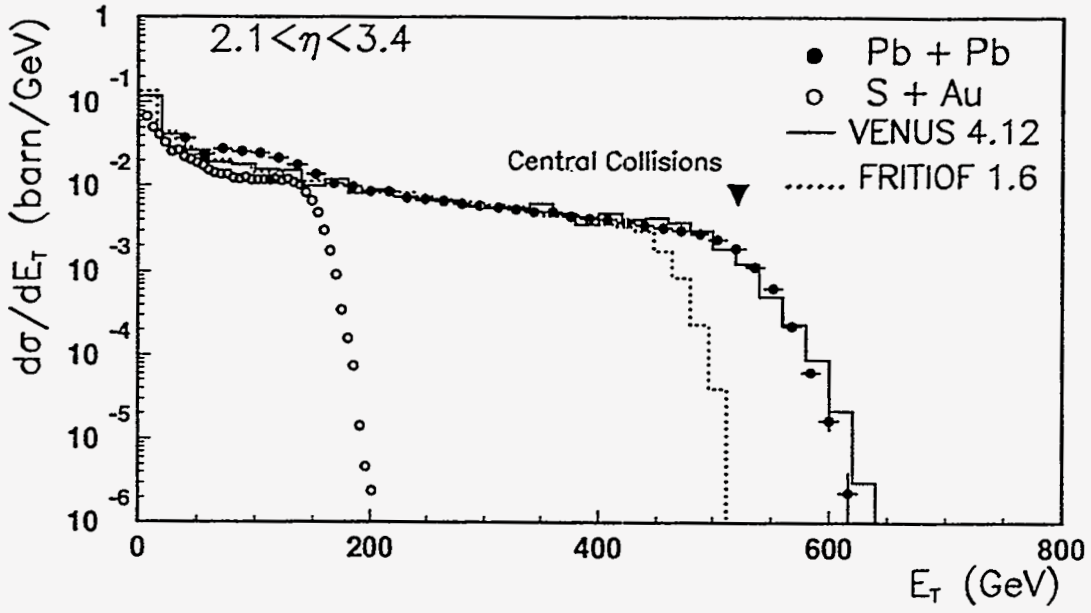

Figure 4. Differential cross section distributions of the transverse energy produced in the collisions, as measured by the Ring calorimeter in the pseudorapidity region $2.1 < \eta < 3.4$. FRITIOF and the VENUS calculations are also shown. For an explanation of the (▼) see text.

depositing 2 TeV of energy in the Veto. This represents only 30% of the $< E_{VETO}^{b\sim 0} > \approx 6$ TeV. From this we conclude that in central Pb+Pb collisions about 70% of the Veto energy is due to forward–going produced particles.

The projection of Fig. 2 onto the E_T axis for the entire data sample gives the transverse energy differential cross section distribution shown in Fig. 4. The shape of the spectrum can again be understood in terms of the collision geometry. In the same figure the predictions of FRITIOF and VENUS are shown as well as the S+Au NA35 data, properly rescaled to the same acceptance. Unlike the case of the E_{VETO} spectrum where both models reproduce the observed distributions, their predictions of the E_T spectrum differ significantly, up to 20% on the tails of the distribution. One major difference in the models which might affect E_T production is the secondary interaction of the produced particles. This is not included in the FRITIOF model but it is contained in the VENUS model, which more closely reproduces the data.

The ▼ in Fig. 4 denotes the mean E_T value in near head-on collisions ($E_T^{b=0}$), calculated in a geometrical manner according to [4]. We find it to be $E_T^{b=0} = 521.5$ GeV which gives $\Delta E_T/\Delta\eta = 401$. We now use Bjorken's formula [5] $\varepsilon = (dE_T/d\eta)/(\pi R^2 \tau)$ in order to calculate the energy densities reached in these collisions, where R is the projectile radius ($R = 1.12 \cdot A^{1/3}$) and τ the formation time, which is put to its nominal value of $\tau = 1$ fm. The resulting energy density is $\varepsilon = 3.0$ GeV/fm^3. This value is similar to the corresponding result in S+Au collisions at the slightly higher projectile energy of 200 GeV/nucleon. We observe that under these assumptions the energy density of

an average central collision does not increase with increasing projectile mass, but the reaction volume increases by a factor of about 3.5. Also, the resulting energy density is approximately 18 times higher than the ground state energy density of nuclear matter ($0.16\,\mathrm{GeV/fm^3}$) and is in the range where deconfinement is predicted.

Transverse energy production can be used to estimate the degree of nuclear stopping achieved in a collision, i.e. the fraction of the projectile energy deposited in the reaction volume. Full stopping is achieved when the incoming projectile nucleons redistribute randomly in space their initial energy through collisions with target nucleons. Thus, the final state particles are expected to be isotropically emitted in the c.m. frame. We choose to define *relative stopping* S to be the ratio $S=E_T/E_T^{max}$ of the observed E_T production to E_T^{max} produced in a full stopping scenario. The latter (E_T^{max}) is essentially the available c.m. energy minus the mass of the participants, multiplied by $\pi/4$ for E_T [4], i.e. $E_T^{max} = (\pi/4) \cdot [\sqrt{s_{TOT}} - m_{part}]$. Taking into account the fact that there are about 2x13 spectators for central Pb+Pb collisions. $E_T^{max} = 2358\,\mathrm{GeV}$. Before we calculate the ratios, we extrapolate the measured data to 4π acceptance. The extrapolation factors derived from FRITIOF and VENUS differ slightly (2.7 and 2.5, respectively). Using the mean value of 2.6 we find $S_{PbPb} = 0.57 \pm 0.05$, which is very close to the corresponding value (0.52) for the S+Au system [4]. Therefore, there is no evidence for a significant change in the stopping for the heavier projectile.

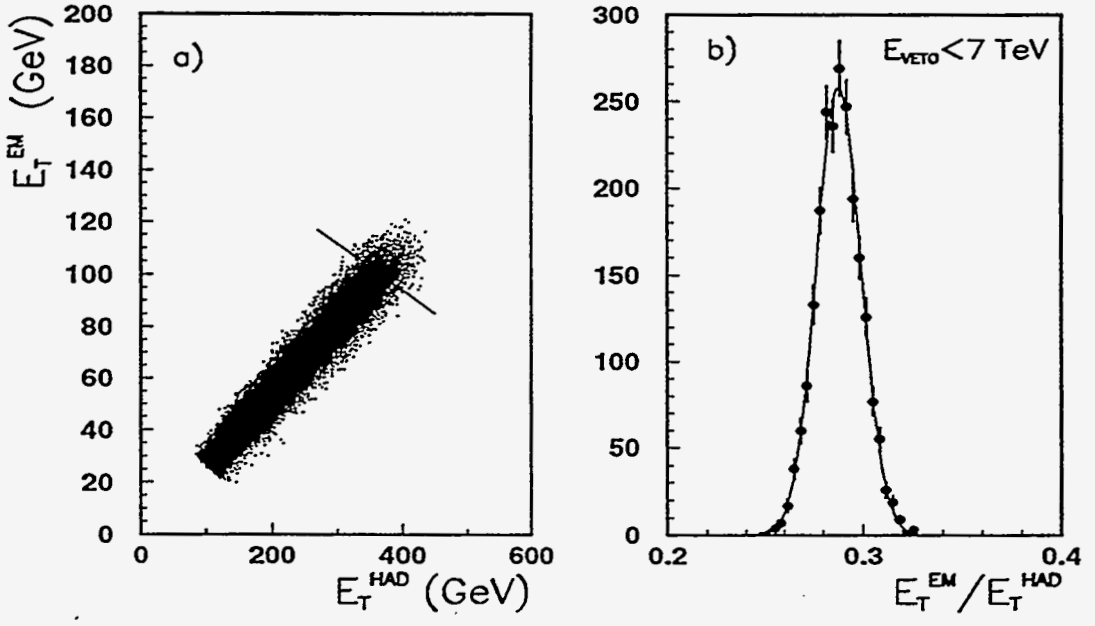

Figure 5. a) the correlation of E_T^{EM} and E_T^{HAD}, and b) the ratio E_T^{EM}/E_T^{HAD} for events with $E_{VETO} < 7\,\mathrm{TeV}$ (preliminary).

Looking at the individual components of the E_T, namely the electromagnetic (mostly γ's from π^0 decays) and the hadronic transverse energy (mostly $\pi^{\pm}$, p and n), we should keep in mind that the unfolding procedure and the large systematic error do not allow

for single event studies. Figure 5a shows a scatter plot of the two components, E_T^{EM} versus E_T^{HAD}. The cut at the lower values is an off-line cut which removes the part of the spectrum which is contaminated by non–target interactions. The two quantities are smoothly correlated without any observable 'abnormal' behavior.

We studied the ratio E_T^{EM}/E_T^{HAD} for an ensemble of central collisions selected by requiring the energy seen by the Veto calorimeter to be less than 7 TeV. The line in Fig. 5a shows the high E_T^{EM}, E_T^{HAD} region from which these events are selected. We show the resulting plot of this ratio in Fig. 5b. The important feature of this distribution, which is not affected by the above–mentioned systematic uncertainties, is the absence of non–statistical variations of E_T^{EM}/E_T^{HAD} away from the mean on both sides of the distribution. The mean value of the distribution is $0.29 \pm .8^{(2)}$ as compared to 0.33 (0.34) in the FRITIOF (VENUS) calculations. The data can be described by a gaussian function with a width $\sigma = 0.011$, which is narrower that the VENUS calculated width of $\sigma = 0.025$. We understand this difference as a systematic effect of the average calculation procedure for the E_T^{EM},E_T^{HAD}.

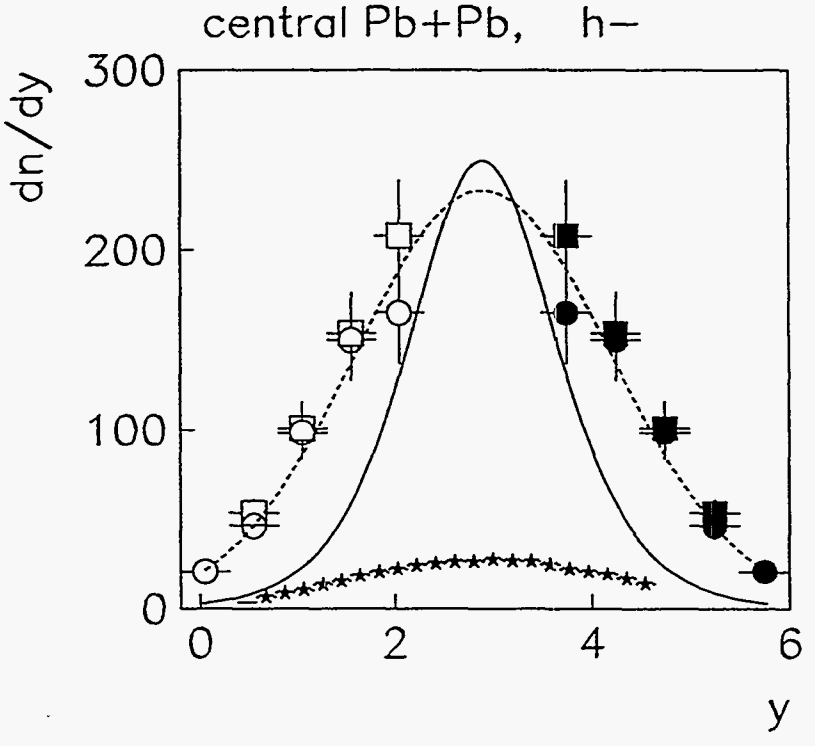

Figure 6. Preliminary rapidity density distributions for h^-, assuming the pion mass, produced in central Pb+Pb collisions at 158 GeV/nucleon. The solid symbols are the actual measurements from the VTP2 (circles) and MTPC (squares). For an explanation of the other symbols see text.

Finally we show some preliminary results [7] from the two tracking devices of the experiment, the MTPC and the VTPC2. Rapidity distributions of negatively charged hadrons, assuming the pion mass and corrected for geometrical acceptance, are shown in

[2]The large systematic error is the result of the (correlated) systematic errors of the individual values.

Fig. 6. The measured points in the experiment are the solid symbols in the high rapidity region. The symmetry of the Pb+Pb system allows for a reflection of the distribution around midrapidity (open symbols). We observe that the results from both TPCs are in close agreement and that the rapidity density in central Pb+Pb collisions peaks at about 230 negative hadrons per unit of rapidity. Also shown (filled stars) is the S+S distribution as measured in NA35[6]. The dashed line is a gaussian fit to the data and the solid line (not normalized to total multiplicity) is the expected width in the case of isotropically emitted pions in the c.m. The experimentally observed distributions for both S+S and Pb+Pb have a FWHM of 3.2±0.4. This is much wider than expected for the isotropic distribution suggesting that this extreme is not achieved. The similar widths of the distributions[3] in S+S and Pb+Pb suggest that rescattering processes among the participating nucleons, which are very different in S+S than in the heavy Pb+Pb system, have little effect on the rapidity distribution of negative hadrons. Preliminary results on Bose–Einstein correlations (HBT effect) are presented in [8].

4. Summary

First (preliminary) results on E_T and hadron production in Pb+Pb collisions using the NA49 apparatus are presented. The analysis indicates that:

- The stopping power is independent of the projectile mass in nucleus–nucleus collisions at the SPS energy.
- Similar energy densities are achieved in Pb+Pb and S+Au collisions, but over a much larger volume for the heavier system.
- Large non-statistical fluctuations in the ratio of electromagnetic to hadronic E_T are not observed.
- Preliminary rapidity density distributions exhibit a non-isotropic distribution of the produced particles in the c.m. frame.

5. Acknowledgments

This work was supported by the Director, Office of Energy Research, Division of Nuclear Physics of the Office of High Energy and Nuclear Physics of the U.S. Department of Energy under Contract DE-AC03-76SF00098, the Bundesministerium für Forschung und Technologie, Germany, the Research Secretariat of the University of Athens, the Polish State Committee for Scientific Research, the Polish–German Foundation, the Hungarian Research Secretariat and EPSRC, U.K., under various grants.

REFERENCES

1. C. de Marzo et al.; NIM 217 (1983) 405
2. I. Huang, S. Margetis, P. Seyboth and D. Vranic; LBL report 36877 (1995)
3. S. Margetis; Ph.D. Thesis, Frankfurt 1990, GSI-91-04

[3]The width is the same even in nucleon–nucleon collisions at the same energy.

4. J. Bächler et al.; Z. Phys. C52(1991)239
5. J.D. Bjorken; Phys. Rev. D27(1983)140
6. J. Bächler et al.; Phys. Rev. Lett. 72(1994)1419
7. M. Gaździcki for the NA35 Collaboration, these proceedings.
8. T. Alber for the NA35 Collaboration, these proceedings.